

Contribution of Ryugu-like material to Earth's volatile inventory by Cu and Zn isotopic analysis

Received: 28 June 2022

Accepted: 27 October 2022

Published online: 12 December 2022

 Check for updates

A list of authors and their affiliations appears at the end of the paper

Initial analyses showed that asteroid Ryugu's composition is close to CI (Ivuna-like) carbonaceous chondrites (CCs) – the chemically most primitive meteorites, characterized by near-solar abundances for most elements. However, some isotopic signatures (for example, Ti, Cr) overlap with other CC groups, so the details of the link between Ryugu and the CI chondrites are not yet fully clear. Here we show that Ryugu and CI chondrites have the same zinc and copper isotopic composition. As the various chondrite groups have very distinct Zn and Cu isotopic signatures, our results point at a common genetic heritage between Ryugu and CI chondrites, ruling out any affinity with other CC groups. Since Ryugu's pristine samples match the solar elemental composition for many elements, their Zn and Cu isotopic compositions likely represent the best estimates of the solar composition. Earth's mass-independent Zn isotopic composition is intermediate between Ryugu/CC and non-carbonaceous chondrites (NCs), suggesting a contribution of Ryugu-like material to Earth's budgets of Zn and other moderately volatile elements.

Ivuna-type (CI) carbonaceous chondrites (CCs) have elemental abundances that are the closest to the composition of the solar photosphere (for example, ref. ¹) (the exceptions being H, C, N, O, Li and the noble gases). Thus, the CIs are key reference samples for investigating how early Solar System processes shaped the compositions of the planets and their building blocks. The return of the Hayabusa2 spacecraft in December 2020, after two successful touchdown and sampling events on the Cb-type asteroid (162173) Ryugu^{2,3}, offers the unprecedented opportunity to study volatile element fractionation processes using samples unaffected by terrestrial alteration, in particular water incorporation. Initial studies on bulk chemical and isotopic compositions revealed similarities between Ryugu and CIs^{4–7}. However, Ryugu samples show slightly higher $\Delta^{17}\text{O}$ than the average from other CI samples, Orgueil and Ivuna, which is interpreted in terms of original heterogeneity between small samples, or contamination of the meteorites by terrestrial water incorporated into the structure of the alteration minerals (for example, phyllosilicates, sulfates, iron oxides and hydroxides), not adsorbed to the surfaces⁵. Similarly, although Ti and Cr isotope compositions show

that asteroid Ryugu formed in the CC reservoir, it was not possible to establish a clear genetic link to just one of the CC groups because the Cr and Ti isotopic compositions of Ryugu overlap not only with CI but also with the Bencubbin-like⁵, Renazzo-like⁵ and high-iron groups. However, the low volatile contents of these three groups of meteorites, as well as the metal-rich nature of the Bencubbin-like and high-iron chondrites, argue against any affinity with Ryugu^{5,6}. Thus, because CI chondrites and Ryugu samples share the same Ti and Cr nucleosynthetic signatures, as well as similar mineralogical and elemental compositions^{5,6}, it has been proposed that they formed contemporaneously from the same outer Solar System reservoir^{3,5–7}.

Material akin to CCs such as Ryugu and the parent body of the CIs could have delivered notable fractions of the moderately and highly volatile elements present in inner Solar System planets (for example, refs. ^{8–13}). Because Ryugu samples have been handled carefully to avoid possible contamination, they are ideally suited to estimate the solar composition and assess the contribution of these outer Solar System objects to the inventory of volatile elements in the terrestrial

✉ e-mail: paquet@ipgp.fr; moynier@ipgp.fr

Table 1 | Zinc and copper stable isotopic compositions of Ryugu samples and carbonaceous chondrites

Sample	Type	<i>n</i> ^a (Zn)	$\delta^{66}\text{Zn}$ (‰)	2s.d. ^b	$\delta^{67}\text{Zn}$ (‰)	2s.d. ^b	$\delta^{68}\text{Zn}$ (‰)	2s.d. ^b	$\epsilon^{66}\text{Zn}$	2s.e. ^b	<i>n</i> ^a (Cu)	$\delta^{65}\text{Cu}$ (‰)	2s.d. ^b
Ryugu													
C0108 ^c		8	0.44	0.05	0.70	0.10	0.91	0.09	-0.21	0.17	5	0.00	0.08
Rpt		6	0.44	0.05	0.60	0.05	0.79	0.09	0.35	0.10			
C0107		8	0.42	0.06	0.57	0.10	0.75	0.09	0.37	0.11			
Rpt		6	0.41	0.05	0.60	0.10	0.76	0.13	0.29	0.11			
<i>Average site C</i>		20	0.43	0.05	0.62	0.13	0.81	0.17	0.34	0.06	5	0.00	0.08
A0106-A107		8	0.45	0.02	0.62	0.06	0.80	0.05	0.42	0.10	3	0.09	0.05
Rpt		6	0.41	0.06	0.59	0.08	0.75	0.11	0.33	0.03			
A0106		8	0.43	0.03	0.63	0.07	0.80	0.06	0.25	0.14			
Rpt		6	0.41	0.06	0.58	0.07	0.76	0.11	0.31	0.05			
<i>Average site A</i>		28	0.43	0.04	0.61	0.08	0.78	0.08	0.33	0.05	3	0.09	0.05
<i>Average Ryugu</i>		48	0.43	0.05	0.61	0.11	0.79	0.14	0.33	0.04	8	0.04	0.11
Carbonaceous Chondrites													
Orgueil	CI1	8	0.52	0.06	0.67	0.11	0.91	0.06	0.62	0.15	2	0.06	0.11
Rpt		8	0.52	0.09	0.71	0.09	0.96	0.17	0.33	0.14			
<i>Average Orgueil</i>		16	0.52	0.08	0.69	0.11	0.94	0.14	0.52	0.12	2	0.06	0.11
Alais	CI1	8	0.45	0.07	0.62	0.11	0.82	0.08	0.35	0.19	2	0.17	0.03
Rpt		6	0.44	0.07	0.62	0.10	0.80	0.12	0.35	0.09			
<i>Average Alais</i>		14	0.45	0.07	0.62	0.10	0.82	0.10	0.35	0.11	2	0.17	0.003
Tagish Lake	C2-ung	8	0.43	0.02	0.55	0.12	0.74	0.06	0.53	0.08			
Rpt		6	0.41	0.08	0.54	0.08	0.73	0.15	0.41	0.07			
<i>Average Tagish Lake</i>		14	0.42	0.06	0.55	0.10	0.73	0.11	0.48	0.06			
Tarda	C2-ung	8	0.46	0.06	0.58	0.09	0.80	0.06	0.50	0.12	1	-0.40	
Rpt		6	0.46	0.09	0.64	0.14	0.83	0.15	0.41	0.08			
<i>Average Tarda</i>		14	0.46	0.07	0.60	0.13	0.81	0.11	0.46	0.08	1	-0.40	
Murchison	CM2	8	0.38	0.03	0.52	0.09	0.70	0.06	0.25	0.13	2	-0.58	0.12
Rpt		6	0.37	0.08	0.52	0.09	0.67	0.15	0.35	0.16			
<i>Average Murchison</i>		14	0.38	0.05	0.52	0.09	0.69	0.10	0.29	0.10	2	-0.58	0.12
Allende A	CV3	5	0.21	0.03	0.26	0.09	0.37	0.08	0.28	0.17	2	-0.80	0.08
Rpt		6	0.22	0.10	0.28	0.16	0.35	0.20	0.47	0.15			
<i>Average Allende A</i>		11	0.22	0.07	0.27	0.13	0.36	0.15	0.38	0.12	2	-0.80	0.08
Allende B	CV3	8	0.24	0.07	0.30	0.14	0.43	0.09	0.23	0.12			
Rpt		6	0.23	0.06	0.31	0.12	0.38	0.18	0.32	0.13			
<i>Average Allende B</i>		14	0.24	0.06	0.31	0.13	0.41	0.14	0.27	0.09			
Reference materials													
IRMM 3702		7	0.22	0.04	0.26	0.05	0.43	0.06	0.02	0.11			
BHVO-2		12	0.30	0.07	0.46	0.08	0.58	0.10	-0.07	0.15			

^a*n* is the number of measurements ^b2s.d. is 2× standard deviation; 2s.e. is 2× standard error ^cValue excluded from the averages for Ryugu Zn isotopic ratios Numbers in italic represent averages for Ryugu and the CCs for the Zn data.

planets. Highly volatile and moderately volatile elements are defined as elements with 50% condensation temperatures (T_c) <665 K and 665–1,135 K, respectively, under canonical nebular gas conditions at 10^{-4} bar (for example, ref. ¹⁴). Zinc and Cu are ideal elements to investigate volatility-related processes, such as volatile element loss, during planetary accretion¹⁵, and are classified as moderately volatile elements (with T_c of 726 K and 1,037 K, respectively)^{14,16}. CC groups display distinct Zn and Cu isotopic mass fractionation effects (for example, refs. ^{17–21}), defining a trend from CIs to CKs (CK, Karoonda-like), with the CIs being the most volatile-rich and isotopically heaviest (for both Zn

and Cu) of the CC groups. We have measured the Zn and Cu isotopic compositions of Ryugu samples to (1) verify the link between Ryugu and CI chondrites for moderately volatile elements, and (2) assess the contribution of Ryugu-like material to the inventory of moderately volatile elements in Earth.

Results

The Zn and Cu isotope compositions for four Ryugu samples (Methods), together with six CC samples (Alais (CI), Allende A and B (CV), Murchison (CM), Orgueil (CI), Tagish Lake (C2-ungrouped) and

Tarda (C2-ungrouped)), were determined following the same analytical protocol and on the same samples as in ref.⁵ (Table 1). Most of these CC samples have previously been characterized for their Zn and Cu isotopic composition^{17–19,21}, except Tarda. The isotopic compositions are given as the permil deviations from the JMC-Lyon Zn and NIST SRM976 Cu standards:

$$\delta^x\text{Zn} = \left[\frac{\left(\frac{x\text{Zn}}{64\text{Zn}} \right)_{\text{Sample}}}{\left(\frac{x\text{Zn}}{64\text{Zn}} \right)_{\text{JMC-Lyon}}} - 1 \right] \times 1000 \quad (1)$$

where $x = 66, 67$ and 68 .

$$\delta^{65}\text{Cu} = \left[\frac{\left(\frac{65\text{Cu}}{63\text{Cu}} \right)_{\text{Sample}}}{\left(\frac{65\text{Cu}}{63\text{Cu}} \right)_{\text{SRM976}}} - 1 \right] \times 1000. \quad (2)$$

During the course of this study, the two standards gave $\delta^{66}\text{Zn}$ of $0.00 \pm 0.005\%$ (2 s.e.; $n = 163$; JMC-Lyon) and $\delta^{65}\text{Cu}$ of $0.00 \pm 0.02\%$ (2 s.e.; $n = 54$; NIST SRM976). Zinc isotope measurements are also corrected for mass-dependent fractionation using the exponential law²², with the normalizing ratio of $^{68}\text{Zn}/^{64}\text{Zn}$ of 0.3856 (ref.²³). Zinc isotopic anomalies are quantified using the epsilon notation relative to the JMC-Lyon standard, as follows:

$$\epsilon^{66}\text{Zn}_c = \left[\frac{\left(\frac{66\text{Zn}}{64\text{Zn}} \right)_{\text{Sample}}}{\left(\frac{66\text{Zn}}{64\text{Zn}} \right)_{\text{JMC-Lyon}}} - 1 \right] \times 10^4 \quad (3)$$

where c is the normalizing ratio $^{68}\text{Zn}/^{64}\text{Zn}$.

The Ryugu samples span a very limited range of mass-dependent Zn isotopic compositions with $\delta^{66}\text{Zn}$ from $+0.41 \pm 0.06$ to $+0.45 \pm 0.02\%$ (2 s.d.), with an average value of $+0.43 \pm 0.05\%$ (2 s.d., $n = 48$) (Fig. 1a and Table 1). The $\delta^{65}\text{Cu}$ values for Ryugu samples range from 0.00 ± 0.08 to $+0.09 \pm 0.05\%$, (average value of $+0.04 \pm 0.11\%$, $n = 8$, 2 s.d.) (Fig. 1b and Table 1). Zinc and Cu abundances also span limited ranges from 338 ± 4 to 383 ± 6 ppm (average 361 ± 40 ppm, $n = 4$, 2 s.d.), and from 133 ± 2 to 168 ± 1 ppm (average 147 ± 37 ppm, $n = 4$, 2 s.d.), respectively (Table 2). These values are higher than the abundances reported for any CI chondrite, consistent with other element abundances for Ryugu samples relative to CIs (Fig. 1, and Table 2), although Ryugu samples have lower H_2O contents than CIs⁵. It is worth noting that the samples from both landing sites show identical $\delta^{66}\text{Zn}$ values (Fig. 1a). In addition, the soluble organic matter extractions of samples C0107 and A0106, which were done before purification of Zn and Cu, do not seem to have affected the Zn and Cu isotope compositions of the Ryugu samples (Methods). All the CCs measured in this study have $\delta^{66}\text{Zn}$ and $\delta^{65}\text{Cu}$ values, as well as Zn and Cu abundances, which are consistent with previous studies (for example, refs.^{17–21}), except for the Cu isotopic composition for Allende A, which is more similar to COs (Ornans-like chondrites) (Figs. 1b and 2). We note, however, that until now only one other measurement of Allende has been reported in the literature¹⁹, and so the difference could represent heterogeneity in the different analysed fractions of Allende in this study and in ref.¹⁹. Similar sample heterogeneities for Cu isotopic compositions have been reported for several fragments of Orgueil²¹. The Ryugu samples exhibit Zn and Cu isotopic compositions that are similar to the Alais and Orgueil samples analysed in this study (Figs. 1 and 2). This is consistent with previous work on the bulk elemental, isotopic and mineralogical properties of these samples, which reveals a genetic link between the Ryugu samples and CI chondrites, implying formation from the same outer Solar System reservoir^{4–6}.

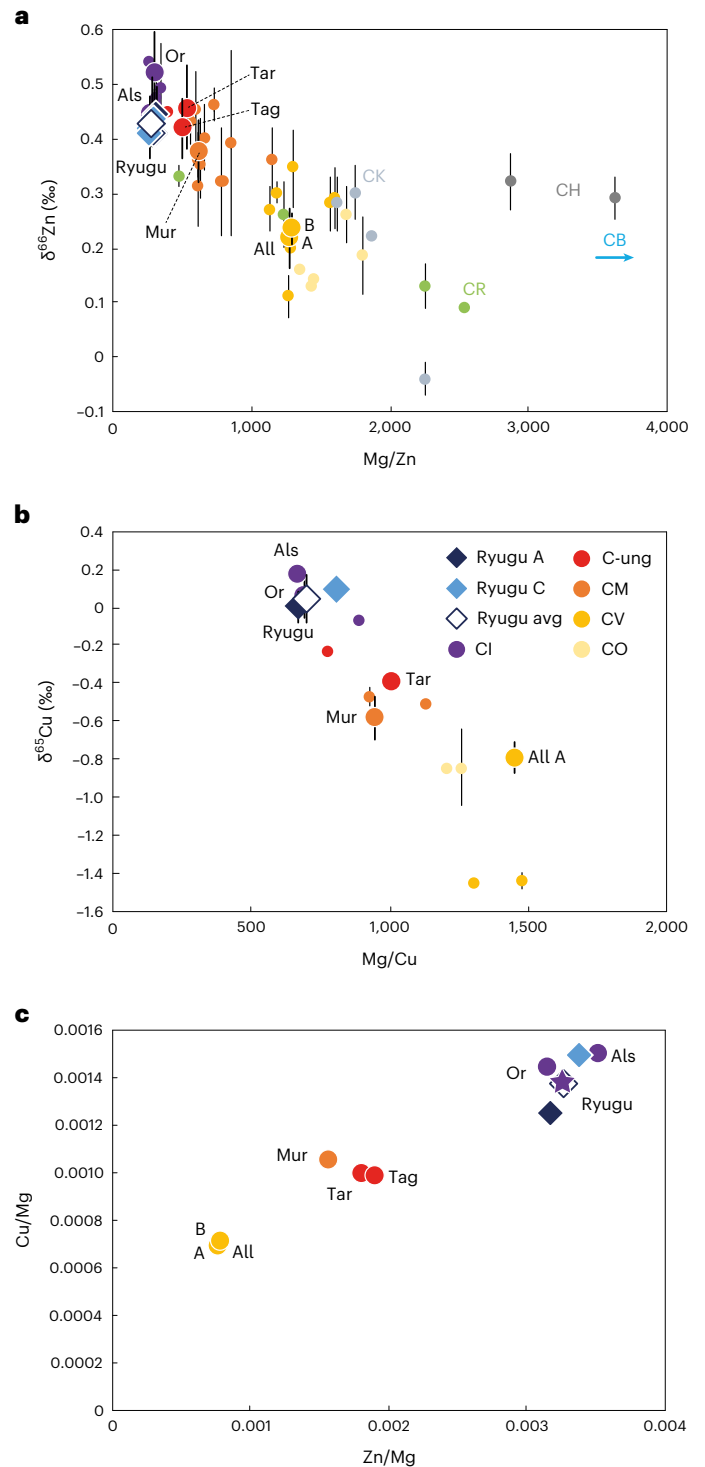


Fig. 1 | Zinc and copper elemental and isotopic compositions for Ryugu and carbonaceous chondrite samples. **a**, $\delta^{66}\text{Zn}$ versus Mg/Zn . **b**, $\delta^{65}\text{Cu}$ versus Mg/Cu . **c**, Zn/Mg versus Cu/Mg that we measured for the Ryugu samples (diamonds) and CCs (large circles with abbreviations: Or, Orgueil; Als, Alais; Tag, Tagish Lake; Tar, Tarda; Mur, Murchison; All, Allende). Small circles are from the literature^{17–21} for Zn and Cu isotope compositions (and references therein for major and trace element compositions). The colour identifies the type of chondrite as described in the legend. The purple star in **c** represents the CI composition from ref.¹. Data are presented as mean values with 2 s.d. error bars, reported in Table 1.

Discussion

Earlier work has shown that bulk CC chondrites define negative correlations in plots of $\delta^{66}\text{Zn}$ versus $1/\text{Zn}$ (refs.^{17,18}) and $\delta^{65}\text{Cu}$ versus

Table 2 | Major and trace element compositions of Ryugu samples and carbonaceous chondrites

Sample	Type	Zn (ppm)	2s.d.	Cu (ppm)	2s.d.	Mg (ppm)	2s.d.	Mg/Zn	Mg/Cu
Ryugu									
C0108*		352	4	156	2	104,222	1,153	296	668
C0107		383	6	168	1	98,823	2,890	258	589
<i>Average site C</i>		368	45	162	17	101,523	7,635	277	628
A0106-A107*		338	4	133	2	106,866	1,250	316	804
A0106		369	5	130	2	112,899	3,191	306	870
<i>Average site A</i>		354	45	132	5	109,883	8,533	311	837
<i>Average Ryugu</i>		361	40	147	37	101,509	11,700	294	733
Carbonaceous Chondrites									
Orgueil	CI1	288	4	131	1	91,158	2,706	317	696
Alais	CI1	298	3	127	1	84,683	2,489	284	667
Tagish Lake	C2-ung	204	5	105	3	107,210	1,275	525	1,021
Tarda	C2-ung	201	3	110	2	111,296	2,388	554	1,012
Murchison	CM2	174	2	117	1	111,130	1,257	637	950
Allende A	CV3	110	2	97	2	141,784	2,461	1289	1,459
Allende B	CV3	121	1	105	1	157,609	4,882	1300	1,501

*Abundances from ref. ⁵ Numbers in italic represent averages for Ryugu, and each of the Ryugu sample sites.

1/Cu (ref. ¹⁹). The variable degree of volatile element depletion among the different CC groups reflect mixing of chemically and isotopically distinct reservoirs during their accretion (for example, refs. ^{17,19,24,25}). The CI chondrites, along with Ryugu, are the least volatile depleted and isotopically heaviest (for both Zn and Cu) of the CC groups, while the most volatile depleted chondrites, the CVs (Vigarano-type chondrites), are the isotopically lightest (this study, refs. ^{17–21}) (Figs. 1 and 2). The CC trend is interpreted as the result of mixing of volatile-rich material enriched in heavy Zn and Cu isotopes and volatile-poor material enriched in light Zn and Cu isotopes (for example, refs. ^{17,19}). Similar correlations are observed for other moderately volatile elements in CCs, such as Te (ref. ²⁵) and Rb (refs. ^{26,27}) and their associated isotope compositions, which is interpreted as mixing between matrix (volatile-rich) and chondrules (volatile-poor) (for example, refs. ^{17,19,24,26}). Such mixing between distinct CC reservoirs is also observed in the relationships between $\delta^{66}\text{Zn}$ and nucleosynthetic isotope anomalies, such as $\epsilon^{54}\text{Cr}$ (parts per ten thousand mass-independent variations of the $^{54}\text{Cr}/^{52}\text{Cr}$ ratio relative to a terrestrial standard) (Fig. 3) (for example, ref. ¹⁸). Ryugu and the CIs have similar Cu and Zn mass-dependent isotopic compositions and differ markedly from the Bencubbin-like and high-iron types (Figs. 1–3). We can, therefore, exclude any genetic relationship to the Bencubbin-like or high-iron groups for the Ryugu samples. A shared nucleosynthetic heritage between Ryugu and CI chondrites has been established on the basis of their identical Ti and Cr nucleosynthetic isotope anomalies^{5,6}. Our Zn and Cu results show that this parentage extends to mass-dependent fractionation of moderately volatile elements, strengthening the link between CI chondrites and Ryugu (Figs. 1–3). The near-solar Zn and Cu relative abundances of Ryugu samples, which are free of the potential ambiguities of terrestrial alteration, suggest that the Zn and Cu isotopic compositions measured for Ryugu and the CI chondrites most probably preserved the proto-Sun's composition¹ (Fig. 1c).

Our study also provides evidence for mass-independent Zn isotope variations ($\epsilon^{66}\text{Zn}$) in Ryugu samples (Fig. 4 and Table 1). These Zn isotopic anomalies are consistent with previous observations^{28,29}. While non-carbonaceous chondrites (NCs) display negative $\epsilon^{66}\text{Zn}$ (ordinary chondrites: $-0.21 \pm 0.04\text{‰}$, 2 s.e., $n = 12$, refs. ^{28,29}; enstatite chondrites $-0.19 \pm 0.08\text{‰}$, 2 s.e., $n = 8$, refs. ^{28,29}), the Ryugu samples and all CCs

exhibit identical positive $\epsilon^{66}\text{Zn}$ within error ($+0.33 \pm 0.04\text{‰}$, 2 s.e., with $n = 7$ for Ryugu (Table 1) and $+0.39 \pm 0.07\text{‰}$, 2 s.e., $n = 7$ for CCs, respectively) with the value previously reported for CC of $+0.28 \pm 0.04\text{‰}$ (2 s.e., $n = 11$)^{28,29}. It is worth noting that the first replicate of sample C0108 (measured at 100 ppb Zn) has an $\epsilon^{66}\text{Zn}$ of $-0.21 \pm 0.17\text{‰}$, whereas the second C0108 replicate (measured at 250 ppb Zn) has an $\epsilon^{66}\text{Zn}$ of $+0.35 \pm 0.10\text{‰}$ similar to all other Ryugu samples (Methods): the first replicate is thus considered an outlier as it was analysed at the lower concentration of 100 ppb and was excluded from the mean value reported here. The reference geological material BHVO-2 and the Zn standard solution IRMM 3702 measured during the first and second sessions have $\epsilon^{66}\text{Zn}$ values ($-0.07 \pm 0.15\text{‰}$, 2 s.e., $n = 12$; $+0.02 \pm 0.11\text{‰}$, 2 s.e., $n = 7$, respectively) consistent within error with estimates for bulk Earth ($+0.015 \pm 0.075\text{‰}$, 2 s.e., $n = 4$, ref. ²⁸ and $-0.07 \pm 0.013\text{‰}$, 2 s.e., $n = 3$, ref. ²⁹). There are no known terrestrial processes that can mass-independently fractionate Zn isotopes. The positive $\epsilon^{66}\text{Zn}$ values in the Ryugu samples, therefore, reinforce their genetic link with the CCs (Fig. 4). Thus, the difference between the CCs and NCs, originally identified in O and Cr isotope compositions³⁰, and later with Ti, Ni and Mo anomalies^{31–36}, appears to also hold for Zn isotopes.

Because meteorites show a large variability of isotope anomalies³⁷ and planetary accretion is stochastic^{38,39}, it is likely that Earth's composition does not reflect accretion from a single type of material, both in terms of isotopic and elemental compositions. Although enstatite chondrites are isotopically closest to the Earth⁴⁰, their chemical signatures are extreme and deviate substantially from the bulk composition of Earth. Possible mixtures of primitive and thermally processed meteorites or their components (for example, chondrules^{6,41–43}) have been proposed to explain the chemical and isotope composition of the Earth^{32,37,44–48}. In particular, the mass-independent isotopic composition of Zn of the Earth appears intermediate between CCs and NCs. Thus, our new data show that CC-like materials, potentially akin to Ryugu, have probably contributed to the delivery of Zn, and more generally volatile elements, to the Earth. Thus, following the same approach as in refs. ^{28,29}, and using the average $\epsilon^{66}\text{Zn} = +0.33 \pm 0.04\text{‰}$ for Ryugu, $+0.35 \pm 0.13\text{‰}$ for CI (this study and refs. ^{28,29}), $-0.20 \pm 0.04\text{‰}$ (2 s.e., $n = 20$) for NCs (ordinary, enstatite from refs. ^{28,29}) and $-0.02 \pm 0.04\text{‰}$ for the bulk silicate earth (BSE) (2 s.e., $n = 7$, refs. ^{28,29}), the mass fraction of Ryugu- or

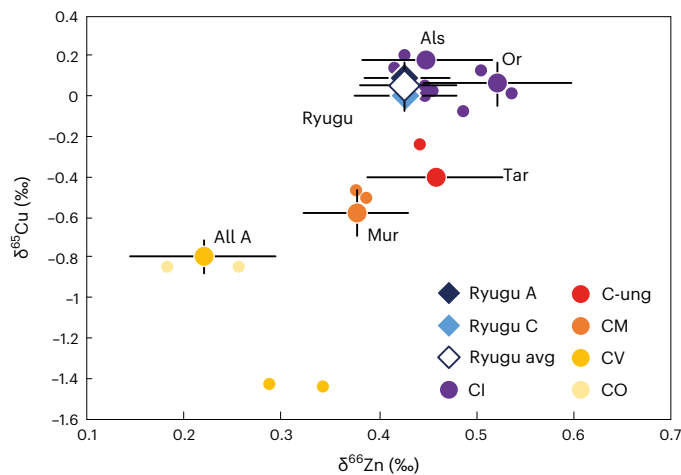


Fig. 2 | $\delta^{66}\text{Zn}$ versus $\delta^{65}\text{Cu}$ for Ryugu samples and carbonaceous chondrites. Literature data are from refs. ^{17,19}. Same symbols as in Fig. 1 for the samples analysed in this study. Other chondrite groups from the literature are reported directly on the figure. Data are presented as mean values with 2 s.d. error bars, reported in Table 1. For clarity, only the error bars of our measurements are displayed. Error bars for literature data are not shown.

CI-derived Zn in the BSE is estimated 33.5 or 32.2%, respectively. Thus, we find that roughly 30% of the terrestrial Zn derives from outer Solar System material, while the NC reservoir contributes to roughly 70% to the terrestrial Zn. Then, to account for the Zn abundances of the accreting materials by Earth, we estimate the mass fractions of NCs and Ryugu-like or CI-like bodies accreted by Earth using the Zn abundance of the BSE of 53.5 ± 2.7 ppm (ref. ⁴⁹), and the $[\text{Zn}]_{\text{Ryugu}}$ of 361 ± 40 ppm (this study) and $[\text{Zn}]_{\text{CI}}$ of 309 ± 43.8 ppm (this study and refs. ^{17,18,21}). Thus, -5% of Ryugu-like material (or -6% of CI-like material) might have contributed to the Earth's mass in order to account for its Zn isotopic composition, which is consistent with previous estimations based on Zn isotopic anomalies^{28,29} and which represents a substantial contribution to the terrestrial budget of moderately volatile elements^{11,28,29}.

Methods

Major and trace elements

Zinc and copper isotopic compositions were measured in four samples from the asteroid (162173) Ryugu (C0108, C0107, A0106-A0107 and A0106). Fragments A0106-A0107 and A0106 came from the first touchdown site, and C0108 and C0107 from the second touchdown site^{4–6}. Samples A0106-A0107 and C0108 were pristine samples, whereas A0106 and C0107 were treated for soluble organic matter (SOM) extraction before chemical purification (Supplementary Table 1). In addition, six CCs (Alais, Allende A, Allende B, Murchison, Orgueil, Tagish Lake and Tarda) were processed following the exact same protocol as the Ryugu samples and were analysed as controls. For each sample, ~25 mg of powder was dissolved at Tokyo Institute of Technology. Elemental abundances were determined using inductively coupled-plasma mass spectrometry: major and trace elements for A0106-A0107 and C0108 samples came from ref. ⁵. After chemical analysis, the same sample solutions were used to determine Zn and Cu isotopic compositions: Zn fractions were pre-separated, as well as 3% of the bulk rock dissolution for Cu purification that represent about 80–100 ng of Cu.

Zinc and copper purification

All the CC meteorites (except Tarda) have previously been measured for Cu and Zn isotopic compositions and were analysed as controls. Further chemical purifications of Zn and Cu on the same sample aliquots were conducted at the Institut de Physique du Globe de Paris (IPGP), using

the procedure described by ref. ⁵⁰ for Zn and by refs. ^{51,52} for Cu. For Zn, samples were loaded in 1.5 mol.L^{-1} HBr on 50 μL of AG1-X8 (200–400 mesh) anion exchange resin in home-made PTFE (polytetrafluoroethylene) columns. Matrix elements were washed by further addition of 2 mL of 1.5 mol.L^{-1} HBr, and Zn was eluted using 2 mL of 0.5 mol.L^{-1} HNO_3 . The collected samples were then evaporated to dryness. For Cu, samples were loaded in 1 mL of 7 mol.L^{-1} HCl on home-made PTFE columns filled with 1.6 mL of AG-MPI resin. After washing the resin with 8 mL of 7 mol.L^{-1} HCl, the Cu was collected with 16 mL of 7 mol.L^{-1} HCl. Both procedures were repeated twice to ensure clean Zn and Cu fractions. The procedural blank was <0.3 ng of Zn and 0.6 ng of Cu, which was negligible relative to the amount of Zn and Cu in the sample mass analysed for the Ryugu samples and the CCs.

Zinc and Cu measurements

Zinc and Cu isotope compositions were determined using a Neptune Plus multi-collector inductively coupled-plasma mass spectrometer at IPGP, using sample-standard bracketing for instrumental mass bias correction as in ref. ⁵⁰ for Zn and refs. ^{51,52} for Cu. Each replicate was analysed 6–8 times for Zn and 1–5 times for Cu depending on the amount of Cu available for each sample, and the reported errors were the two standard deviations (2 s.d.) of these repeated measurements. For the Zn measurements, the samples were analysed in two sessions with different sample solution concentrations: one at 100 ppb of Zn and a second one at 250 ppb of Zn, with an uptake of $100 \mu\text{L.min}^{-1}$. For the Cu measurements, the samples were analysed in one session at a concentration of 30 ppb of Cu with the same uptake. The high purity of the final Zn fraction was needed to remove isobaric and non-isobaric interferences from the signal. Interference on ^{64}Zn by ^{64}Ni was corrected by measuring the intensity of the ^{62}Ni , assuming natural abundances of Ni isotopes ($^{62}\text{Ni} = 3.63\%$; $^{64}\text{Ni} = 0.93\%$). No N_2 was used during the measurements as this results in high background on mass 68 from ArN_2 . No interference on mass 68.5 from Ba^{2+} was detected during the sessions. The reference geological material BHVO-2 and the Zn standard solution IRMM 3702 measured during the first and second sessions gave values consistent with the literature (for example, refs. ^{18,20}). However, during the first session, the Zn fractions were measured at 100 ppb of Zn. All the Ryugu and CC samples had similar positive $\epsilon^{66}\text{Zn}$, except for the first replicate of sample C0108 that had a negative value. In other words, all the samples plot below the mass-dependent equilibrium fractionation line in a $\delta^{66}\text{Zn}$ against $\delta^{65}\text{Zn}$ plot, whereas the C0108

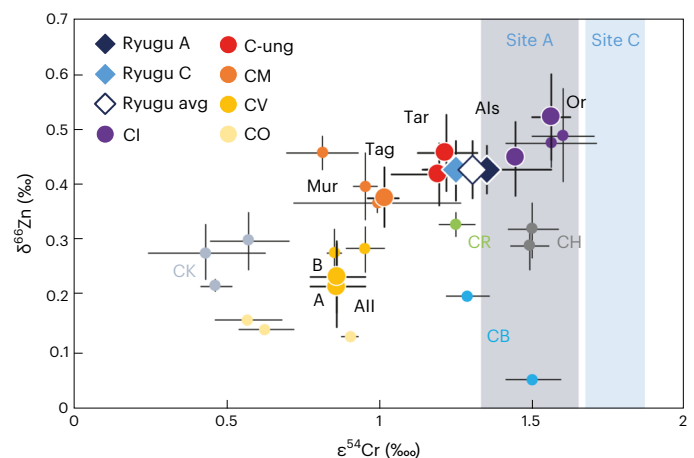


Fig. 3 | $\delta^{66}\text{Zn}$ (this study) versus $\epsilon^{54}\text{Cr}$ (refs. ^{5,30,53–55}) for Ryugu samples and carbonaceous chondrites. Literature data are from refs. ^{17,18,20} for Zn isotope compositions, and from ref. ⁵⁶ for Cr isotope compositions. The dark and light blue shaded areas correspond to the $\epsilon^{54}\text{Cr}$ ranges for site A and site C, respectively, from ref. ⁶. Same symbols as in Fig. 1 for the samples analysed in this study. Other chondrite groups from the literature are reported directly on the figure. Data are presented as mean values with 2 s.d. error bars, reported in Table 1.

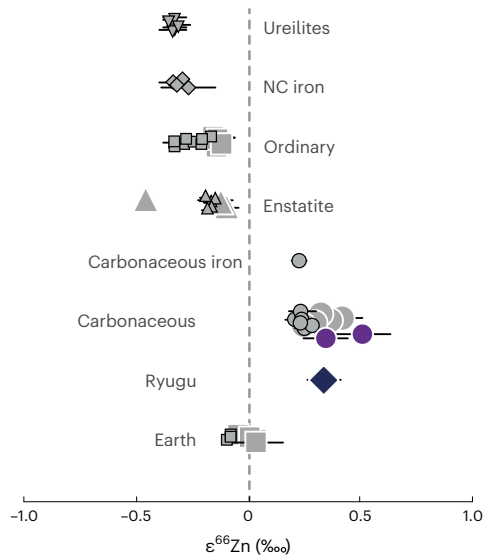


Fig. 4 | Variations of $\epsilon^{66}\text{Zn}$ among different groups of meteorites. For comparison purposes, only Ryugu (diamond) and CI (purple circles) samples measured in this study are represented here. Literature data for CCs (ref. ²⁸ shown with large symbols, ref. ²⁹ shown with small symbols), ordinary chondrites^{28,29}, enstatite chondrites^{28,29}, NC and CC iron chondrites²⁹, and ureilites²⁹ are shown with grey symbols. Bulk silicate earth: $+0.015 \pm 0.075\text{‰}$, 2 s.e., $n = 4$, ref. ²⁸ and $-0.07 \pm 0.013\text{‰}$, 2 s.e., $n = 3$, ref. ²⁹. Data are presented as mean values with 2 s.e. error bars, reported in Table 1.

replicate falls above it (Supplementary Fig. 1a). This motivated our second session of measurements on replicates at higher concentrations (250 ppb of Zn) to ensure that the observed $\epsilon^{66}\text{Zn}$ values were not analytical artefacts. The second replicate of sample C0108, analysed at 250 ppb of Zn, shows the same isotopic signature as the rest of the Ryugu sample set and plots below the mass-dependent fractionation line with a positive $\epsilon^{66}\text{Zn}$ (Supplementary Fig. 1b). In the discussion and associated figures, only the second replicate of sample C0108 is considered and represented.

Data availability

All data referred to in this article can be found in the tables or source data. Source data are provided with this paper.

References

- Lodders, K. Relative atomic solar system abundances, mass fractions, and atomic masses of the elements and their isotopes, composition of the solar photosphere, and compositions of the major chondritic meteorite groups. *Space Sci. Rev.* **217**, 44 (2021).
- Morota, T. et al. Sample collection from asteroid (162173) Ryugu by Hayabusa2: implications for surface evolution. *Science* **368**, 654–659 (2020).
- Tachibana, S. et al. Pebbles and sand on asteroid (162173) Ryugu: in situ observation and particles returned to Earth. *Science* **375**, 1011–1016 (2022).
- Yada, T. et al. Preliminary analysis of the Hayabusa2 samples returned from C-type asteroid Ryugu. *Nat. Astron.* **6**, 214–220 (2022).
- Yokoyama, T. et al. The first returned samples from a C-type asteroid show kinship to the chemically most primitive meteorites. *Science* <https://doi.org/10.1126/science.abn7850> (2022).
- Nakamura, E. et al. On the origin and evolution of the asteroid Ryugu: a comprehensive geochemical perspective. *Proc. Jpn Acad. Ser. B Phys. Biol. Sci.* **98**, 227–282 (2022).
- Ito, M. et al. A pristine record of outer Solar System materials from asteroid Ryugu's returned sample. *Nat. Astron.* **6**, 1163–1171 (2022).
- Wang, Z. & Becker, H. Ratios of S, Se and Te in the silicate Earth require a volatile-rich late veneer. *Nature* **499**, 328–331 (2013).
- Savage, P. S. et al. Copper isotope evidence for large-scale sulphide fractionation during Earth's differentiation. *Geochem. Perspect. Lett.* <https://doi.org/10.7185/geochemlet.1506> (2015).
- Schönbächler, M., Carlson, R. W., Horan, M. F., Mock, T. D. & Hauri, E. H. Heterogeneous accretion and the moderately volatile element budget of Earth. *Science* **328**, 884–887 (2010).
- Braukmüller, N., Wombacher, F., Funk, C. & Münker, C. Earth's volatile element depletion pattern inherited from a carbonaceous chondrite-like source. *Nat. Geo.* **12**, 564–568 (2019).
- Varas-Reus, M. I., König, S., Yierpan, A., Lorand, J. P. & Schoenberg, R. Selenium isotopes as tracers of a late volatile contribution to Earth from the outer Solar System. *Nat. Geo.* **12**, 779–782 (2019).
- Kubik, E. et al. Tracing Earth's volatile delivery with tin. *J. Geophys. Res. Solid Earth* **126**, e2021JB022026 (2021).
- Lodders, K. Solar system abundances and condensation temperatures of the elements. *ApJ* **591**, 1220 (2003).
- Day, J. M. & Moynier, F. Evaporative fractionation of volatile stable isotopes and their bearing on the origin of the Moon. *Phil. Trans. RSA* **372**, 20130259 (2014).
- Schaefer, L. & Fegley, B. Jr Chemistry of atmospheres formed during accretion of the Earth and other terrestrial planets. *Icarus* **208**, 438–448 (2010).
- Luck, J. M., Othman, D. B. & Albarède, F. Zn and Cu isotopic variations in chondrites and iron meteorites: early solar nebula reservoirs and parent-body processes. *Geochim. Cosmochim. Acta* **69**, 5351–5363 (2005).
- Pringle, E. A., Moynier, F., Beck, P., Paniello, R. & Hezel, D. C. The origin of volatile element depletion in early solar system material: Clues from Zn isotopes in chondrules. *Earth Planet. Sci. Lett.* **468**, 62–71 (2017).
- Luck, J. M., Othman, D. B., Barrat, J. A. & Albarède, F. Coupled ^{63}Cu and ^{16}O excesses in chondrites. *Geochim. Cosmochim. Acta* **67**, 143–151 (2003).
- Mahan, B., Moynier, F., Beck, P., Pringle, E. A. & Siebert, J. A history of violence: Insights into post-accretionary heating in carbonaceous chondrites from volatile element abundances, Zn isotopes and water contents. *Geochim. Cosmochim. Acta* **220**, 19–35 (2018).
- Barrat, J. A. et al. Geochemistry of CI chondrites: major and trace elements, and Cu and Zn isotopes. *Geochim. Cosmochim. Acta* **83**, 79–92 (2012).
- Rosman, K. J. R. A survey of the isotopic and elemental abundance of zinc. *Geochim. Cosmochim. Acta* **36**, 801–819 (1972).
- Russell, W. A., Papanastassiou, D. A. & Tombrello, T. A. Ca isotope fractionation on the Earth and other solar system materials. *Geochim. Cosmochim. Acta* **42**, 1075–1090 (1978).
- Clayton, R. N. & Mayeda, T. K. Oxygen isotope studies of carbonaceous chondrites. *Geochim. Cosmochim. Acta* **63**, 2089–2104 (1999).
- Hellmann, J. L., Hopp, T., Burkhardt, C. & Kleine, T. Origin of volatile element depletion among carbonaceous chondrites. *Earth Planet. Sci. Lett.* **549**, 116508 (2020).
- Pringle, E. A. & Moynier, F. Rubidium isotopic composition of the Earth, meteorites, and the Moon: evidence for the origin of volatile loss during planetary accretion. *Earth Planet. Sci. Lett.* **473**, 62–70 (2017).
- Nie, N. X. et al. Imprint of chondrule formation on the K and Rb isotopic compositions of carbonaceous meteorites. *Sci. Adv.* **7**, eabl3929 (2021).

28. Savage, P. S., Moynier, F. & Boyet, M. Zinc isotope anomalies in primitive meteorites identify the outer solar system as an important source of Earth's volatile inventory. *Icarus* **386**, 115172 (2022).
29. Steller, T., Burkhardt, C., Yang, C. & Kleine, T. Nucleosynthetic zinc isotope anomalies reveal a dual origin of terrestrial volatiles. *Icarus* **386**, 115171 (2022).
30. Trinquier, A., Birck, J. L. & Allègre, C. J. Widespread ⁵⁴Cr heterogeneity in the inner solar system. *ApJ* **655**, 1179 (2007).
31. Trinquier, A. et al. Origin of nucleosynthetic isotope heterogeneity in the solar protoplanetary disk. *Science* **324**, 374–376 (2009).
32. Warren, P. H. Stable-isotopic anomalies and the accretionary assemblage of the Earth and Mars: a subordinate role for carbonaceous chondrites. *Earth Planet. Sci. Lett.* **311**, 93–100 (2011).
33. Budde, G. et al. Molybdenum isotopic evidence for the origin of chondrules and a distinct genetic heritage of carbonaceous and non-carbonaceous meteorites. *Earth Planet. Sci. Lett.* **454**, 293–303 (2016).
34. Kruijjer, T. S., Burkhardt, C., Budde, G. & Kleine, T. Age of Jupiter inferred from the distinct genetics and formation times of meteorites. *Proc. Natl Acad. Sci. USA* **114**, 6712–6716 (2017).
35. Burkhardt, C., Dauphas, N., Hans, U., Bourdon, B. & Kleine, T. Elemental and isotopic variability in solar system materials by mixing and processing of primordial disk reservoirs. *Geochim. Cosmochim. Acta* **261**, 145–170 (2019).
36. Nanne, J. A., Nimmo, F., Cuzzi, J. N. & Kleine, T. Origin of the non-carbonaceous–carbonaceous meteorite dichotomy. *Earth Planet. Sci. Lett.* **511**, 44–54 (2019).
37. Dauphas, N. et al. Calcium-48 isotopic anomalies in bulk chondrites and achondrites: evidence for a uniform isotopic reservoir in the inner protoplanetary disk. *Earth Planet. Sci. Lett.* **407**, 96–108 (2014).
38. Chambers, J. E. Planetary accretion in the inner Solar System. *Earth Planet. Sci. Lett.* **223**, 241–252 (2004).
39. Walsh, K. J., Morbidelli, A., Raymond, S. N., O'Brien, D. P. & Mandell, A. M. A low mass for Mars from Jupiter's early gas-driven migration. *Nature* **475**, 206–209 (2011).
40. Javoy, M. et al. The chemical composition of the Earth: enstatite chondrite models. *Earth Planet. Sci. Lett.* **293**, 259–268 (2010).
41. Morbidelli, A., Libourel, G., Palme, H., Jacobson, S. A. & Rubie, D. C. Subsolar Al/Si and Mg/Si ratios of non-carbonaceous chondrites reveal planetesimal formation during early condensation in the protoplanetary disk. *Earth Planet. Sci. Lett.* **538**, 116220 (2020).
42. Frossard, P., Guo, Z., Spencer, M., Boyet, M. & Bouvier, A. Evidence from achondrites for a temporal change in Nd nucleosynthetic anomalies within the first 1.5 million years of the inner solar system formation. *Earth Planet. Sci. Lett.* **566**, 116968 (2021).
43. Alexander, C. M. D. An exploration of whether Earth can be built from chondritic components, not bulk chondrites. *Geochim. Cosmochim. Acta* **318**, 428–451 (2022).
44. Lodders, K. in *From Dust to Terrestrial Planets* (eds Benz, W. et al.) 341–354 (Springer, 2000).
45. Schiller, M., Bizzarro, M. & Fernandes, V. A. Isotopic evolution of the protoplanetary disk and the building blocks of Earth and the Moon. *Nature* **555**, 507–510 (2018).
46. Schiller, M., Bizzarro, M. & Siebert, J. Iron isotope evidence for very rapid accretion and differentiation of the proto-Earth. *Sci. Adv.* **6**, eaay7604 (2020).
47. Mezger, K., Maltese, A. & Vollstaedt, H. Accretion and differentiation of early planetary bodies as recorded in the composition of the silicate Earth. *Icarus* **365**, 114497 (2021).
48. Johansen, A. et al. A pebble accretion model for the formation of the terrestrial planets in the Solar System. *Sci. Adv.* **7**, eabc0444 (2021).
49. Sossi, P. A., Nebel, O., O'Neill, H. S. C. & Moynier, F. Zinc isotope composition of the Earth and its behaviour during planetary accretion. *Chem. Geol.* **477**, 73–84 (2018).
50. van Kooten, E. & Moynier, F. Zinc isotope analyses of singularly small samples (<5 ng Zn): investigating chondrule-matrix complementarity in Leoville. *Geochim. Cosmochim. Acta* **261**, 248–268 (2019).
51. Moynier, F., Creech, J., Dallas, J. & Le Borgne, M. Serum and brain natural copper stable isotopes in a mouse model of Alzheimer's disease. *Sci. Rep.* **9**, 11894 (2019).
52. Moynier, F. et al. Copper and zinc isotopic excursions in the human brain affected by Alzheimer's disease. *Alzheimer's Dement. Diagn. Assist. Dis. Monit.* **12**, e12112 (2020).
53. Petitat, M., Birck, J. L., Luu, T. H. & Gounelle, M. The chromium isotopic composition of the ungrouped carbonaceous chondrite Tagish Lake. *ApJ* **736**, 23 (2011).
54. Schoenberg, R. et al. The stable Cr isotopic compositions of chondrites and silicate planetary reservoirs. *Geochim. Cosmochim. Acta* **183**, 14–30 (2016).
55. Dey, S., Yin, Q. Z. & Zolensky, M. Exploring the planetary genealogy of Tarda—a unique new carbonaceous chondrite. In *Proc. 52nd Lunar and Planetary Science Conference* no. 2548, 2517 (Lunar and Planetary Institute, 2021).
56. Zhu, K. et al. Chromium isotopic insights into the origin of chondrite parent bodies and the early terrestrial volatile depletion. *Geochim. Cosmochim. Acta* **301**, 158–186 (2021).

Acknowledgements

This work was partly supported by the IPGP analytical platform PARI, Region Ile-de-France SESAME grant no. 12015908, and DIM ACAV+, the European Research Council grant agreement no. 101001282 (METAL) (F.M.), the UnivEarthS Labex programme (grant nos. ANR-10-LABX-0023 and ANR-11-IDEX-0005-02) (F.M.), JSPS Kaken-hi grants (S. Tachibana, H. Yurimoto and T. Yokoyama) and the CNES.

Author contributions

F.M., M.P. and T. Yokoyama designed the project. H. Yurimoto and T. Yokoyama coordinated the isotopic analyses of the samples among members of the Hayabusa2-initial-analysis chemistry team. M.P. and T. Yokoyama processed the samples and separated the Zn and Cu from the matrix. M.P. measured the Zn and Cu isotopic compositions. M.P. and F.M. wrote the first draft of the manuscript, with contributions from T. Yokoyama, W.D., Y. Hu, Y.A., J.A., C.M.O'D.A., S.A., Y.A., K.B., M.B., A.B., R.W.C., M.C., B.-G.C., N.D., A.M.D., T.D.R., W.F., R.F., I.G., M.K.H., Y. Hibiyu, H. Hidaka, H. Homma, P. H., G.R.H., K.I., T.I., T.R.I., A.I., M.I., S.I., N.K., N.T.K., K.K., T.K., S.K., A.N.K., M.-C.L., Y.M., K.D.M., M.M., K.M., I.N., K.N., D.N., A.N.N., L.N., M.O., A.P., C.P., L.P., L.Q., S.S.R., N.S., M.S., L.T., H.T., K.T., Y. Terada, T.U., S.W., M.W., R.J.W., K. Yamashita, Q.-Z.Y., S.Y., E.D.Y., H. Yui, A.-C.Z., T. Nakamura, H.N., T. Noguchi, R.O., K.S., H. Yabuta, M.A., A.M., A.N., M.N., T.O., T. Yada, K. Yogata, S.N., T.S., S. Tanaka, F.T., Y. Tsuda, S.-I.W., M.Y., S. Tachibana and H. Yurimoto.

Competing interests

The authors declare no competing interests.

Additional information

Supplementary information The online version contains supplementary material available at <https://doi.org/10.1038/s41550-022-01846-1>.

Correspondence and requests for materials should be addressed to Marine Paquet or Frederic Moynier.

Peer review information *Nature Astronomy* thanks Herbert Palme, Katharina Lodders and the other, anonymous, reviewer(s) for their contribution to the peer review of this work.

Reprints and permissions information is available at www.nature.com/reprints.

Publisher's note Springer Nature remains neutral with regard to jurisdictional claims in published maps and institutional affiliations.

Springer Nature or its licensor (e.g. a society or other partner) holds exclusive rights to this article under a publishing agreement with the author(s) or other rightsholder(s); author self-archiving of the accepted manuscript version of this article is solely governed by the terms of such publishing agreement and applicable law.

© The Author(s), under exclusive licence to Springer Nature Limited 2022, corrected publication 2023

Marine Paquet ¹✉, **Frederic Moynier** ¹✉, **Tetsuya Yokoyama**², **Wei Dai**¹, **Yan Hu** ¹, **Yoshinari Abe**³, **Jérôme Aléon**⁴, **Conel M. O'D. Alexander** ⁵, **Sachiko Amari** ⁶, **Yuri Amelin**⁷, **Ken-ichi Bajo** ⁸, **Martin Bizzarro**^{1,9}, **Audrey Bouvier** ¹⁰, **Richard W. Carlson** ⁵, **Marc Chaussidon**¹, **Byeon-Gak Choi** ¹¹, **Nicolas Dauphas** ¹², **Andrew M. Davis** ¹², **Tommaso Di Rocco**¹³, **Wataru Fujiya** ¹⁴, **Ryota Fukai** ¹⁵, **Ikshu Gautam** ², **Makiko K. Haba** ², **Yuki Hibiya**¹⁶, **Hiroshi Hidaka**¹⁷, **Hisashi Homma** ¹⁸, **Peter Hoppe**¹⁹, **Gary R. Huss** ²⁰, **Kiyohiro Ichida** ²¹, **Tsuyoshi Iizuka**²², **Trevor R. Ireland** ²³, **Akira Ishikawa**², **Motoo Ito** ²⁴, **Shoichi Itoh** ²⁵, **Noriyuki Kawasaki**⁸, **Noriko T. Kita** ²⁶, **Kouki Kitajima** ²⁶, **Thorsten Kleine** ²⁷, **Shintaro Komatani** ²¹, **Alexander N. Krot** ²⁰, **Ming-Chang Liu**²⁸, **Yuki Masuda** ², **Kevin D. McKeegan** ²⁸, **Mayu Morita** ²¹, **Kazuko Motomura**²⁹, **Izumi Nakai**³⁰, **Kazuhide Nagashima** ²⁰, **David Nesvorný** ³¹, **Ann N. Nguyen** ³², **Larry Nittler** ⁵, **Morihiko Onose**²¹, **Andreas Pack**¹³, **Changkun Park** ³³, **Laurette Piani** ³⁴, **Liping Qin** ³⁵, **Sara S. Russell**³⁶, **Naoya Sakamoto** ³⁷, **Maria Schönbächler** ³⁸, **Lauren Tafra**²⁸, **Haolan Tang**²⁸, **Kentaro Terada** ³⁹, **Yasuko Terada**⁴⁰, **Tomohiro Usui** ¹⁵, **Sohei Wada**⁸, **Meenakshi Wadhwa**⁴¹, **Richard J. Walker** ⁴², **Katsuyuki Yamashita** ⁴³, **Qing-Zhu Yin** ⁴⁴, **Shigekazu Yoneda** ⁴⁵, **Edward D. Young**²⁸, **Hiroharu Yui**⁴⁶, **Ai-Cheng Zhang** ⁴⁷, **Tomoki Nakamura**⁴⁸, **Hiroshi Naraoka** ⁴⁹, **Takaaki Noguchi** ²⁴, **Ryuji Okazaki**⁴⁹, **Kanako Sakamoto** ¹⁵, **Hikaru Yabuta** ⁵⁰, **Masanao Abe**¹⁵, **Akiko Miyazaki** ¹⁵, **Aiko Nakato**¹⁵, **Masahiro Nishimura**¹⁵, **Tatsuaki Okada** ¹⁵, **Toru Yada** ¹⁵, **Kasumi Yogata** ¹⁵, **Satoru Nakazawa** ¹⁵, **Takanao Saiki**¹⁵, **Satoshi Tanaka**¹⁵, **Fuyuto Terui**⁵¹, **Yuichi Tsuda**¹⁵, **Sei-ichiro Watanabe** ¹⁷, **Makoto Yoshikawa**¹⁵, **Shogo Tachibana** ⁵² & **Hisayoshi Yurimoto** ⁸

¹Université Paris Cité, Institut de Physique du Globe de Paris, CNRS, Paris, France. ²Department of Earth and Planetary Sciences, Tokyo Institute of Technology, Tokyo, Japan. ³Graduate School of Engineering Materials Science and Engineering, Tokyo Denki University, Tokyo, Japan. ⁴Institut de Minéralogie, de Physique des Matériaux et de Cosmochimie, Sorbonne Université, Muséum National d'Histoire Naturelle, CNRS UMR 7590, IRD, Paris, France. ⁵Earth and Planets Laboratory, Carnegie Institution for Science, Washington, DC, USA. ⁶McDonnell Center for the Space Sciences and Physics Department, Washington University, St. Louis, MO, USA. ⁷Guangzhou Institute of Geochemistry, Chinese Academy of Sciences, Guangzhou, China. ⁸Natural History Sciences, IIL, Hokkaido University, Sapporo, Japan. ⁹Centre for Star and Planet Formation, GLOBE Institute, University of Copenhagen, Copenhagen, Denmark. ¹⁰Bayerisches Geoinstitut, Universität Bayreuth, Bayreuth, Germany. ¹¹Department of Earth Science Education, Seoul National University, Seoul, Republic of Korea. ¹²Department of the Geophysical Sciences and Enrico Fermi Institute, The University of Chicago, Chicago, IL, USA. ¹³Faculty of Geosciences and Geography, University of Göttingen, Göttingen, Germany. ¹⁴Faculty of Science, Ibaraki University, Mito, Japan. ¹⁵ISAS/JSEC, JAXA, Sagami-hara, Japan. ¹⁶General Systems Studies, The University of Tokyo, Tokyo, Japan. ¹⁷Earth and Planetary Sciences, Nagoya University, Nagoya, Japan. ¹⁸Osaka Application Laboratory, SBUWDX, Rigaku Corporation, Osaka, Japan. ¹⁹Max Planck Institute for Chemistry, Mainz, Germany. ²⁰Hawai'i Institute of Geophysics and Planetology, University of Hawai'i at Mānoa, Honolulu, HI, USA. ²¹Analytical Technology, Horiba Techno Service Co., Ltd, Kyoto, Japan. ²²Earth and Planetary Science, The University of Tokyo, Tokyo, Japan. ²³School of Earth and Environmental Sciences, The University of Queensland, St Lucia, Queensland, Australia. ²⁴Kochi Institute for Core Sample Research, JAMSTEC, Kochi, Japan. ²⁵Earth and Planetary Sciences, Kyoto University, Kyoto, Japan. ²⁶Geoscience, University of Wisconsin-Madison, Madison, WI, USA. ²⁷Max Planck Institute for Solar System Research, Göttingen, Germany. ²⁸Earth, Planetary, and Space Sciences, UCLA, Los Angeles, CA, USA. ²⁹Thermal Analysis, Rigaku Corporation, Tokyo, Japan. ³⁰Department of Applied Chemistry, Tokyo University of Science, Tokyo, Japan. ³¹Department of Space Studies, Southwest Research Institute, Boulder, CO, USA. ³²Astromaterials Research and Exploration Science, NASA Johnson Space Center, Houston, TX, USA. ³³Earth-System Sciences, Korea Polar Research Institute, Incheon, Korea. ³⁴Centre de Recherches Pétrographiques et Géochimiques, CNRS - Université de Lorraine, Nancy, France. ³⁵CAS Key Laboratory of Crust-Mantle Materials and Environments, University of Science and Technology of China, School of Earth and Space Sciences, Hefei, China. ³⁶Department of Earth Sciences, Natural History Museum, London, UK. ³⁷IIL, Hokkaido University, Sapporo, Japan. ³⁸Institute for Geochemistry and Petrology, Department of Earth Sciences, ETH Zurich, Zurich, Switzerland. ³⁹Earth and Space Science, Osaka University, Osaka, Japan. ⁴⁰Spectroscopy and Imaging, Japan Synchrotron Radiation Research Institute, Hyogo, Japan. ⁴¹School of Earth and Space Exploration, Arizona State University, Tempe, AZ, USA. ⁴²Geology, University of Maryland, College Park, MD, USA. ⁴³Graduate School of Natural Science and Technology, Okayama University, Okayama, Japan. ⁴⁴Earth and Planetary Sciences, University of California, Davis, CA, USA. ⁴⁵Science and Engineering, National Museum of Nature and Science, Tsukuba, Japan. ⁴⁶Chemistry, Tokyo University of Science, Tokyo, Japan. ⁴⁷School of Earth Sciences and Engineering, Nanjing University, Nanjing, China. ⁴⁸Department of Earth Science, Tohoku University, Sendai, Japan. ⁴⁹Department of Earth and Planetary Sciences, Kyushu University, Fukuoka, Japan. ⁵⁰Earth and Planetary Systems Science Program, Hiroshima University, Higashi-Hiroshima, Japan. ⁵¹Kanagawa Institute of Technology, Atsugi, Japan. ⁵²UTokyo Organization for Planetary and Space Science, University of Tokyo, Tokyo, Japan. ✉e-mail: paquet@ipgp.fr; moynier@ipgp.fr